THE JOURNAL OF PHYSICAL CHEMISTRY B

ARTICLE

pubs.acs.org/JPCB

The Nature of the Sodium Dodecylsulfate Micellar Pseudophase as Studied by Reaction Kinetics

Lavinia Onel and Niklaas J. Buurma*

Physical Organic Chemistry Centre, School of Chemistry, Cardiff University, Main Building, Park Place, Cardiff CF10 3AT, United Kingdom

Supporting Information

ABSTRACT: The nature of the rate-retarding effects of anionic micelles of sodium dodecyl sulfate (SDS) on the water-catalyzed hydrolysis of a series of substituted 1-benzoyl-1,2,4-triazoles (**1a**−**f**) has been studied. We show that medium effects in the micellar Stern region of SDS can be reproduced by simple aqueous model solutions containing small-molecule mimics for the surfactant headgroups and tails, namely sodium methyl sulfate (NMS) and 1-propanol, in line with our previous kinetic studies for cationic surfactants (Buurma et al. *J. Org. Chem.* **2004**, *69*, 3899−3906). We have improved our mathematical description leading to the model solution, which has made the identification of appropriate model solutions more efficient. For the Stern region of SDS, the model solution consists of a mixture of 35.3 mol dm^{-3} H_2O, corresponding to an effective water concentration of 37.0 mol dm^{-3}, 3.5 mol dm^{-3} sodium methylsulfate (NMS) mimicking the SDS headgroups, and 1.8 mol dm^{-3} 1-propanol mimicking the backfolding hydrophobic tails. This model solution quantitatively reproduces the rate-retarding effects of SDS micelles found for the hydrolytic probes **1a**−**f**. In addition, the model solution accurately predicts the micropolarity of the micellar Stern region as reported by the $E_T(30)$ solvatochromic probe. The model solution also allows the separation of the individual contributions of local water concentration (water activity), polarity and hydrophobic interactions, ionic strength and ionic interactions, and local charge to the observed local medium effects. For all of our hydrolytic probes, the dominant rate-retarding effect is caused by interactions with the surfactant headgroups, whereas the local polarity as reported by the solvatochromic $E_T(30)$ probe and the Hammett ρ value for hydrolysis of **1a**−**f** in the Stern region of SDS micelles is mainly the result of interactions with the hydrophobic surfactant tails. Our results indicate that both a mimic for the surfactant tails (NMS) and a mimic for the surfactant headgroups (1-propanol) are required in a model solution for the micellar pseudophase to reproduce all medium effects experienced by a variety of different probes.

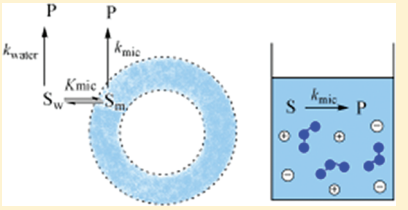

INTRODUCTION

Micelle-forming amphiphiles spontaneously self-aggregate cooperatively above the critical micelle concentration (cmc), forming highly dynamic aggregates. Although different micelles can have different morphologies (which can roughly be predicted from the shape of the constituent surfactants),[1] here, we focus on approximately spherical micelles. For spherical morphology, one of the most commonly accepted models for the micellar structure is that proposed by Gruen.[2] Gruen's model features a rather sharp interface between a dry hydrophobic hydrocarbon core[2−4] and the so-called Stern region. The Stern region is a region filled with surfactant headgroups, some of the counterions (for ionic surfactants), backfolding surfactant tails, and water. The Stern region thus represents an interfacial zone between the hydrocarbon core and bulk water. In line with this division in zones, in the pseudophase formalism,[5] micelles and bulk water are considered to be different reaction regions, exerting different reaction medium effects. As such, taking into account the clear differences between the micellar core and the Stern region, these zones themselves could also be considered as two distinct pseudophases inside the micelles.[6]

The increasing interest over the past several decades in organic reactivity in aqueous solutions has resulted in widespread use of micelles to increase the solubility of hydrophobic compounds in aqueous solutions.[6−10] In micellar solutions, reactions can be either accelerated or decelerated compared to the reactions in aqueous solutions without added cosolutes.[11−13] Remarkable success in enhancing reaction rates has been achieved by applying micelles as catalysts (introducing catalytic moieties in micelle-forming surfactants) and by micelle-assisted catalysis.[11,14−25] In micelle-assisted catalysis, micelles solubilize the reactants and the catalyst, placing them in close proximity inside the small volume of the micellar pseudophase. Although highly effective examples of micelle-assisted catalysis are available, rational design of catalytic systems based on quantitative data remains elusive. One of the principal reasons for this is the fact that kinetic schemes, typically involving at least micellar binding of one or more reactants and the catalyst and local rate constants in the different pseudophases, often become unreliable. In practice, this means that individual parameters, such as the rate constant of a reaction in the micellar pseudophase, cannot be determined or can be determined only with great difficulty, because of strong parameter

Received: August 24, 2011
Revised: September 27, 2011
Published: September 27, 2011

covariance.[26,27] Without access to accurate values for the various parameters, an in-depth analysis of micelle-assisted catalysis is nontrivial, to say the least. To address this situation, reliable model solutions for the micellar pseudophase are required. Such model solutions not only allow the determination of accurate estimates of micellar rate constants, but ideally also provide insight into the factors affecting micellar reactivity. For the development of such model solutions, we limit our discussion to medium effects exerted by micelles of nonfunctionalized amphiphiles on uncatalyzed hydrolysis reactions[28] for which reliable models for data analysis exist.

As discussed above, to understand the micellar acceleration and deceleration of reactions, a good understanding of the micellar pseudophase as a reaction medium is necessary. Although many kinetic studies of micellar medium effects on various organic reactions have already been reported,[6,11,14,15,29,30] the description of the local reaction environment offered by micelles has remained obscure. The present work continues our kinetic studies of micellar effects on the water-catalyzed hydrolysis of a series of activated amides.[31] Previously, we showed that these reactions occur in the micellar Stern region, and our approach therefore leads to a description of the micellar Stern region as a reaction medium.[31,32] An analysis of the reaction medium properties of the Stern region is of wide interest because the majority of reactants used in organic reactions in micellar solutions bind in the micellar Stern region.[6,12,33−35] This preference for the Stern region probably stems from its versatility as a binding location because it contains, in addition to water molecules, highly hydrophilic surfactant headgroups and hydrophobic domains of backfolding surfactant tails.

A characteristic feature of the Stern region of ionic micelles is the high local concentration of headgroups, counterions, and backfolding surfactant tails residing at the micelle interface. Calculations have estimated the concentration of headgroups in the Stern region of spherical ionic micelles to be 1−3 M (Mukerjee[36]), 4−7 M (Bunton et al.[37]), and 2−6 M (Buurma et al.[6]). Methods using molecular spectroscopic probes (such as solvatochromic, fluorescent, and spin-label probes)[38−41] and reactive probes[42,43] have also been used to gain insight into the properties of the micellar interfacial region and its composition. Model solutions for the micellar Stern region were found useful for estimating the interfacial concentrations of water[40−43] and counterions.[42,43] The chemical trapping method developed by Romsted et al.[42,43] for probing the micellar Stern region showed that the concentrations of headgroups and counterions in the interfacial region of micelles of cationic surfactants such as cetyltrimethylammonium bromide and cetyltrimethylammonium chloride fall roughly in the range of 1−3 M. The concentration of counterions is slightly less than the concentration of headgroups because of incomplete counterion binding in the Stern region.

The interface of sodium dodecyl sulfate (SDS) micelles as a reaction medium has previously been modeled using aqueous salt solutions, usually involving sodium methyl sulfate (NMS).[32,44,45] Based on their earlier work, Cuccovia et al.[44] used aqueous solutions containing 1.5 mol dm^{-3} NMS and solutions containing 1.5 mol dm^{-3} sodium methylsulfonate as model solutions for the Stern region of SDS micelles in their chemical trapping experiments when studying the interfacial concentration of coions Cl^- and Br^-. The chemical trapping method was not used to determine the interfacial concentration of SDS headgroups, even though the anionic sulfate group reacts with the arenediazonium ion, because of the instability of the alkyl aryl sulfate ester product, which hydrolyzes rapidly.[43] Buurma et al.[32] and Muñoz and co-workers[45] used a more concentrated salt solution containing 4.3 mol dm^{-3} NMS to model the Stern region of SDS micelles. Using these salt solutions for modeling the interfacial region of SDS micelles showed that it was not possible to reproduce the micellar polarity as reported by the $E_T(30)$ probe.[32] In addition, the inhibition exerted by SDS micelles on phenyl chloroformate hydrolysis was much larger than the rate retardation observed in the model solution.[45] The authors of both studies[45,46] concluded that a better description of micellar effects on the reaction rates includes the contribution of hydrophobic interactions with the backfolding hydrocarbon tails, which is not taken into account using a model solution containing only the headgroup mimic NMS. In our subsequent kinetic study[31] of the interfacial region of micelles of the cationic surfactants dodecyltrimethylammonium bromide (DTAB) and cetyltrimethylammonium bromide (CTAB), we used model solutions containing, in addition to the salt mimicking the surfactant headgroups, 1-propanol as a small-molecule mimic of the hydrocarbon tails. Deconvolution of the rate-retarding effects of micelles of DTAB and CTAB on a series of probe reactions allowed the identification of aqueous model solutions, consisting of mixtures of tetramethylammonium bromide, mimicking micellar headgroups, and 1-propanol, mimicking the backfolding tails, that largely reproduced the observed micellar kinetics. This solution also correctly predicted the $E_T(30)$ value for the CTAB Stern region, highlighting the importance of including hydrophobic interactions in model solutions for the micellar pseudophase.

In the present work, we test the general validity of such modeling for an anionic surfactant, namely, SDS. Our goal is to test whether a concentrated aqueous mixture of the headgroup mimic NMS and the backfolding-tail mimic 1-propanol reproduces the rate-retarding effects of SDS micelles on the hydrolysis of the same series of activated amides as used in ref 31 (**1a**−**f**, Scheme 1). In addition, by improving the mathematical description developed in our earlier work for the identification of the appropriate model solution,[31] we more efficiently achieve a more complete representation of the micellar Stern region as a reaction medium. Using the $E_T(30)$ solvatochromic probe as a micropolarity reporter, we probe the ability of the model solution to predict the medium properties of the interfacial region of SDS micelles that were not included in our kinetic modeling. In line with our previous study, we chose the water-catalyzed pH-independent hydrolysis of different substituted 1-benzoyl-1,2,4-triazoles (**1a**−**f**, Scheme 1) as the probe reaction, because the series of hydrolytic probes **1a**−**f** has the required differences in sensitivity to environment.[31] The reactions occur through a

Scheme 1

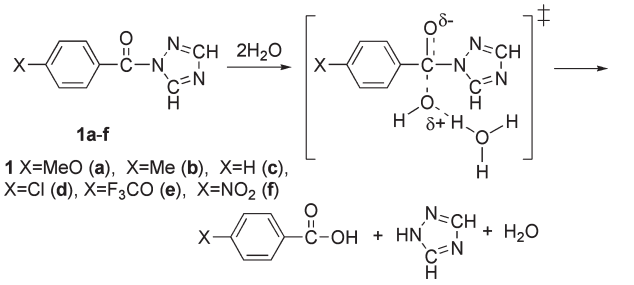

dipolar activated complex involving two molecules of water, one acting as a nucleophile and the other as a general base.[47−49]

EXPERIMENTAL SECTION

Chemicals. Sodium dodecylsulfate (SDS) (99%, Fluka), sodium methylsulfate (NMS) (98%, TCI), *p*-anisoyl chloride (99%, Acros Organics), *p*-toluoyl chloride (99%, Acros Organics), benzoyl chloride (99%, Acros Organics), *p*-chlorobenzoyl chloride (99%, Aldrich), *p*-(trifluoromethyl)benzoyl chloride (98%, Acros Organics), *p*-nitrobenzoyl chloride (99%, Fluka), 1,2,4-triazole (purum, ≥98%, Fluka), *p*-toluic acid (98%, Aldrich), *p*-(trifluoromethyl)benzoic acid (99%, Acros Organics), and Reichardt's $E_T(30)$ dye (90%, Aldrich) were used as received. The substituted 1-benzoyl-1,2,4-triazoles **1a**−**f** were synthesized according to literature procedures.[50]

Spectrophotometric Measurements. Aqueous solutions were prepared in water purified using an ELGA option-R 7BP water purifier. Micellar solutions were acidified (HCl) to roughly pH 5.3. This pH was chosen to achieve conditions of pH-independent reaction in both the bulk water and the micellar pseudophase; the observed rate constant for the hydrolysis of each substituted probe in 100 mM SDS does not change if the pH is a few tenths of a pH unit above or below 5.3, indicating that 5.3 still lies in the range of pH values where the rate constant for hydrolysis is pH-independent in the micellar pseudophase. NMS solutions, 1-propanol solutions, and the model (micelle-mimicking) solutions were acidified to pH 4. The hydrolytic probes were injected as 7 μL of a stock solution of **1a**−**f** in acetonitrile into a 1.00-cm-path-length cuvette containing ca. 2.5 mL of an aqueous solution of interest, yielding a total probe concentration during the reaction of ca. 10^{-5} mol dm^{-3}. The hydrolysis reactions were monitored by parallel kinetic measurements using a JASCO V650 UV−visible spectrophotometer with an AutoPeltier thermostatting unit with six-position cell changer PAC-743R. Reactions were followed at 296, 262, 251.5, 262, 253, and 262 nm for **1a**−**f**, respectively, at 25 °C for at least eight half-lives. The decrease of absorbance with time at the selected wavelengths was reproduced well by the pseudo-first-order kinetics rate law

$$A_t = A_{fin} + \Delta A e^{-k_{obs}t} \quad (1)$$

where A_t is the absorbance at time t, A_{fin} is the final absorbance, ΔA represents the difference between the absorbance at time zero and A_{fin}, and k_{obs} is the observed pseudo-first-order rate constant.

Measurements Involving the $E_T(30)$ Solvatochromic Probe. All spectra were recorded at 25 °C, pH 12. The $E_T(30)$ probe was injected as 14 μL of a stock solution in ethanol into a 1.00-cm-path-length cuvette containing 3.2 mL of an aqueous solution of interest. The UV−visible spectra were recorded using a JASCO V630 spectrophotometer with a JASCO EHC-716 Peltier unit for temperature control.

HPLC Measurements. High-performance liquid chromatography (HPLC) experiments were performed using an Agilent 1200 instrument with a ZORBAX Eclipse XDB-C18 4.6 × 150 mm column. Samples of the reaction mixtures for **1a**−**f** were analyzed as soon as the reactions were finished using the HPLC method described in the Supporting Information.

Error Margins. Error margins for all observed rate constants represent standard deviations around average values. Error margins for micellar rate constants and micellar binding constants were determined by nonlinear least-squares fitting of the Menger−Portnoy equation (vide infra) to the experimental data. Errors were propagated[51] as required. Error margins for the molality of 1-propanol ($m_{1\text{-propanol}}$) and the molality of NMS (m_{NMS}) in solution 1 (Tables 4 and 9) represent standard deviations determined by the singular value decomposition method.[52] To determine the error margins for $m_{1\text{-propanol}}$ and m_{NMS} in solution 2, we added the respective standard deviations to each term ($a'_{X,1\text{-propanol}}$, $a'_{X,NMS}$, $b_{X,1\text{-propanol}}$, $b_{X,NMS}$ and c_X) in eq 11 (vide infra) and also subtracted the respective standard deviations from each term in eq 11. The equation obtained in each of these two cases was solved numerically using the Levenberg−Marquardt method[53] resulting in two "extreme solutions". Taking the two extreme solutions together with the best-fit values for $m_{1\text{-propanol}}$ and m_{NMS} according to the average first and second derivatives, we obtained three sets of molalities for the two mimicking compounds in the model solution. For each mimic, the average of the three molalities coincides with the optimum value of the molality in solution 2 (2.8 mol kg^{-1} for 1-propanol and 5.5 mol kg^{-1} for NMS), indicating that the error margins are symmetric. The error margins for $m_{1\text{-propanol}}$ and m_{NMS} in solution 2 (Table 4) were determined as standard deviations for these sets of three values.

Table 1. Rate Constants for Hydrolysis in Water without Added Cosolutes and in the SDS Micellar Pseudophase and Micellar Binding Constants[a] for Para-Substituted 1-Benzoyl-1,2,4-triazoles 1a−f at 25 °C

probe	σ_p[b]	$k_{X,water}$ (10^{-4} s^{-1})	$k_{X,mic}$ (10^{-4} s^{-1})	$K_{X,mic}$ (10^3 M^{-1})
1a	−0.28	4.04 ± 0.05	0.145 ± 0.002	9.05 ± 0.03
1b	−0.14	9.42 ± 0.01	0.39 ± 0.02	10.07 ± 0.13
1c[c]	0.00	21.00 ± 0.02	1.13 ± 0.06	3.55 ± 0.04
1d	+0.24	36.00 ± 0.02	1.86 ± 0.02	10.37 ± 0.04
1e	+0.32	43.25 ± 0.07	2.60 ± 0.04	18.19 ± 0.15
1f	+0.81	274 ± 8	26.4 ± 2.2	4.55 ± 0.18

[a] Calculated using the Menger−Portnoy equation,[5] with the cmc set to 7.9 mM (determined using isothermal titration calorimetry, in close agreement with values in the literature[55−57]) and an aggregation number of 64.[58] [b] Hammett substituent constants from ref 59. [c] In acceptable agreement with k_{mic} and K_{mic} for **1c** and SDS from Fadnavis et al.[60]

RESULTS AND DISCUSSION

For convenience of data analysis, the kinetic experiments are ideally carried out in the pH range in which the hydrolysis of substituted 1-benzoyl-1,2,4-triazoles (**1a**−**f**) is pH-independent (Scheme 1) in both the aqueous and micellar pseudophases. Based on kinetic measurements for probe **1d** (Figures S1.1 and S1.2, Supporting Information), a bulk pH of 5.3 appeared to provide these ideal conditions. To confirm that a bulk pH of 5.3 is suitable for the other kinetic probes as well, we studied the hydrolysis of **1a**−**f** over a limited range of pH values around 5.3 in the presence of 100 mM SDS and found the observed rate constants to be invariant around this pH. In addition, the observed rate constants for hydrolysis of each probe **1a**−**f** in water without added cosolutes at pH 5.3 (Table 1) are in excellent agreement with those for the corresponding hydrolysis in water at pH 4.[31] The local pH on the surface of SDS micelles is lower than the bulk pH and can be estimated by applying the Poisson−Boltzmann equation[54] that relates the proton activity at the surface of a charged micelle to that in bulk water in

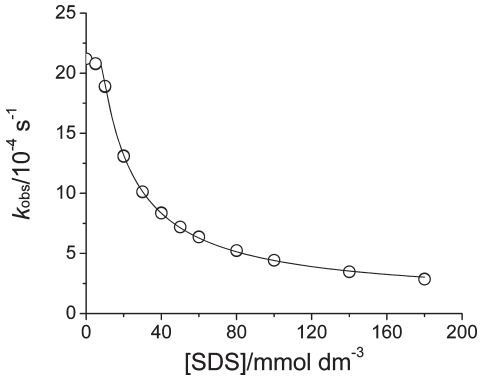

Figure 1. Observed rate constant of hydrolysis of **1c** at 25 °C in solutions containing varying concentrations of SDS at pH 5.3. Experimental data were fitted with eq 2.

combination with the interfacial electrostatic potential. Based on the interfacial potential of −134 mV for SDS micelles,[54] the calculated interfacial pH is approximately 3.0 for a bulk pH of 5.3. We therefore chose a bulk pH of 5.3 for all kinetic experiments.

The hydrolysis reactions of **1a**−**f** all follow pseudo-first-order kinetics. The rate constants for hydrolysis of **1a**−**f** in water without added cosolutes, $k_{X,water}$ (subscript X indicates the substituent of the probe as shown in Scheme 1), are presented in Table 1. The rate constant of hydrolysis increases with increasing electron-withdrawing ability of the substituent, as expected for a reaction in which a partial negative charge develops on the carbonyl group going toward the activated complex.

Next, the effect of micelles on the hydrolysis of **1a**−**f** was studied. For all hydrolytic probes, SDS micelles retard hydrolysis. Figure 1 shows the kinetic profile for **1c**. Kinetic profiles for **1a,b** and **1d**−**f** are shown in Figure S2.1a,b,d−f (Supporting Information).

The kinetic data for hydrolysis of **1a**−**f** in the presence of a range of SDS concentrations at a bulk pH of 5.3 were analyzed using the nonlinear form of the pseudophase model developed by Menger and Portnoy[5] (eq 2). The pseudophase model assumes an equilibrium between free and micelle-bound substrate and makes a distinction between the reaction rate constants in bulk water and in the micellar pseudophase

$$k_{obs} = \frac{k_{water} + k_{mic}K_m([surf] - cmc)/N}{1 + K_m([surf] - cmc)/N} \quad (2)$$

where k_{obs} is the observed pseudo-first-order rate constant defined by eq 1 at a surfactant concentration of [surf], k_{water} is the rate constant in water in the absence of added cosolutes, and k_{mic} is the rate constant under conditions of complete binding of the substrate to the micelles. K_m is the binding constant of the kinetic probe to SDS micelles, cmc is the critical micelle concentration of the surfactant, and N is the average micellar aggregation number. Because all hydrolytic probes **1a**−**f** bind in the micellar interfacial region (vide supra), k_{mic} is the rate constant for hydrolysis in the micellar Stern region.

From a nonlinear least-squares fit of eq 2 to the experimental data, micellar rate constants for hydrolysis and micellar binding constants for SDS were determined (Table 1). The micellar binding constants for **1a**−**f** binding to SDS are similar to the corresponding K_m values for CTAB (Table 2 in ref 31). However, the K_m values for SDS are on average about 3 times larger than those for DTAB.[31]

Table 2. Relative Rate Constants for Hydrolysis of 1a−f in SDS Micelles and Water at 25 °C

probe	$k_{X,mic}/k_{X,water}$	$\ln(k_{X,mic}/k_{X,water})$
1a	0.0359 ± 0.0006	−3.33 ± 0.02
1b	0.041 ± 0.002	−3.18 ± 0.05
1c	0.053 ± 0.003	−2.92 ± 0.05
1d	0.0516 ± 0.0005	−2.96 ± 0.01
1e	0.060 ± 0.001	−2.81 ± 0.01
1f	0.096 ± 0.008	−2.34 ± 0.08

The rate-retarding effects exerted by SDS micelles on the individual hydrolytic probes are described by the micellar rate constants relative to the rate constants in water, that is, $k_{X,mic}/k_{X,water}$, and the natural logarithms of these relative rate constants, $\ln(k_{X,mic}/k_{X,water})$ (Table 2).

The relative rate constants $k_{X,mic}/k_{X,water}$ for **1a**−**f** increase with Hammett substituent constant (σ). Therefore, the rate-retarding effect exerted by SDS micelles on the hydrolysis of **1a**−**f** decreases with increasing electron-withdrawing ability of the substituent. A similar trend was found for the hydrolysis of **1a**−**f** in CTAB and DTAB micelles (Table 3 in ref 31).

There is no significant correlation between the micellar binding constants, $K_{X,mic}$, for **1a**−**f** and the micellar rate constants, $k_{X,mic}$ (Table 1), or between the micellar binding constants, $K_{X,mic}$, for **1a**−**f** and the relative micellar rate constants, $k_{X,mic}/k_{X,water}$ (Table 2). This lack of correlation is in line with the hypothesis that all hydrolytic probes **1a**−**f** bind in the Stern region in the micellar pseudophase and that different rate-retarding effects are not the result of different binding locations within the micelle (vide infra). Micellar rate constants for all probes **1a**−**f** in SDS micelles are 2−3 times smaller than k_{mic} for CTAB and DTAB micelles.[31] The fact that observed k_{mic} values for anionic SDS are lower than for cationic DTAB and CTAB is in agreement with observations by Bunton et al.[61,62] and Campos-Rey et al.[13] regarding the effects of the electrostatic non-neutrality of ionic micelles on reactions involving partial charges in the transition state. Here, the partial negative charge on the carbonyl in the activated complex will be destabilized by the anionic Stern region, whereas with cationic surfactants, a stabilizing effect occurs. To determine whether the additional destabilizing effect exerted on the transition state by the local negative charge of SDS micelles enhances the difference between the effects of electron-donating and electron-withdrawing substituents on the transition state, we constructed Hammett plots[63,64] (Figure S3.1, Supporting Information) for hydrolysis of **1a**−**f** in bulk water and in the micellar pseudophases of SDS, CTAB, and DTAB. The Hammett ρ value equals 1.6 for the reaction in water and is approximately 2.0 for all micelles, independent of the headgroup charge. Therefore, for hydrolysis of **1a**−**f**, the effects exerted by the negatively charged interface of SDS micelles do not depend on the substituent on the hydrolytic probes; otherwise, the Hammett ρ values for anionic and cationic micelles would be different. This finding is in agreement with the effects of the headgroup mimic NMS, which does not strongly affect the Hammett ρ value for hydrolysis of **1a**−**f** (vide infra).

First Model Solution. To obtain a description of the micellar Stern region as a reaction medium, the effects of ionic interactions with the headgroups and hydrophobic interactions with the alkyl tails on the kinetic probes have to be distinguished. We previously[31] achieved such a separation of the kinetic effects

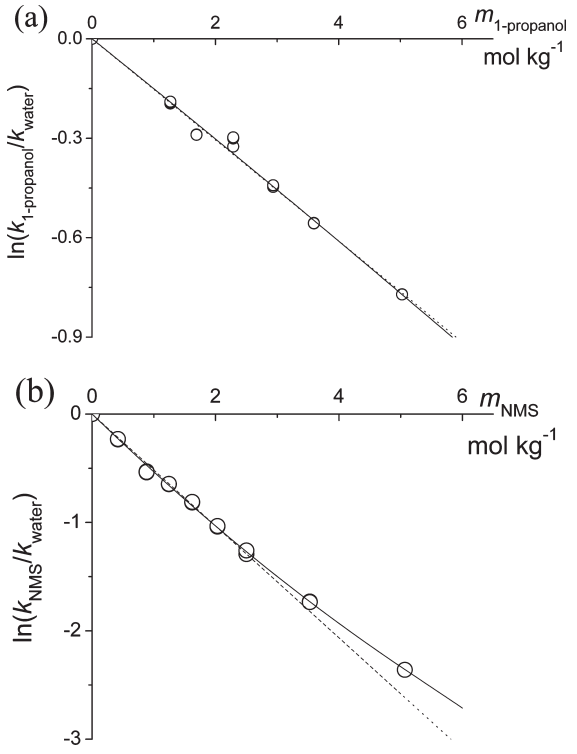

Figure 2. Linear fit (dotted line) and second-order polynomial fit (solid line) of the individual effects of (a) 1-propanol and (b) NMS on the observed rate constant of hydrolysis of probe **1d** at 25 °C versus the (a) 1-propanol molality and (b) NMS molality.

exerted by DTAB and CTAB micelles on hydrolysis of **1a**−**f** using tetramethylammonium bromide (TMAB) as a mimic for the surfactant headgroups and 1-propanol as a mimic for the backfolding surfactant tails. In the present study, the rate-retarding effects of SDS headgroups are mimicked using NMS, and the effects of the hydrocarbon chains are again modeled using 1-propanol. The sensitivities of hydrolytic probes **1a**−**f** to added NMS and 1-propanol were determined separately in the molality range of 0−5 mol kg^{-1} for each mimicking compound. Figure 2 summarizes the kinetic data for **1d**, with data for **1a**−**c**,**e**,**f** in Figures S4.1a−c,e,f and S5.1a−c,e,f (Supporting Information). Using our previously developed approach,[31] we quantify the sensitivities of the hydrolysis rate constants of **1a**−**f** to each modeling compound by the slopes of the logarithms of the relative rate constants, $\ln(k_{X,NMS}/k_{X,water})$ and $\ln(k_{X,1\text{-propanol}}/k_{X,water})$, versus the molality of the cosolute, namely m_{NMS} and $m_{1\text{-propanol}}$. The subscript X again refers to the substituent on the hydrolytic probe. The slopes were obtained by analyzing $\ln(k_{X,NMS}/k_{X,water})$ versus m_{NMS} and $\ln(k_{X,1\text{-propanol}}/k_{X,water})$ versus $m_{1\text{-propanol}}$ in terms of eqs 3 and 4, respectively (Figure 2a,b).

$$\ln\left(\frac{k_{X,\,NMS}}{k_{X,\,water}}\right) = a_{X,\,NMS}m_{NMS} \tag{3}$$

$$\ln\left(\frac{k_{X,\,1\text{-propanol}}}{k_{X,\,water}}\right) = a_{X,\,1\text{-propanol}}m_{1\text{-propanol}} \tag{4}$$

Slopes $a_{X,NMS}$ and $a_{X,1\text{-propanol}}$ (eqs 3 and 4), that is the first-order derivatives of the logarithms of the rate constants relative to those in water as a function of the molalities of NMS and 1-propanol, respectively, reflect the 1:1 interactions, or pairwise interactions, between each cosolute and probes **1a**−**f**,[65,66] and these are summarized in Table 3.

Table 3. Sensitivities of the Rate Constants of Hydrolysis of the Probes 1a−f to 1-Propanol and NMS in Accordance with the Mathematical Description Leading to Solution 1

probe	$a_{X,1\text{-propanol}}$ [a]	$a_{X,NMS}$ [b]
1a	−0.236 ± 0.005	−0.547 ± 0.009
1b	−0.232 ± 0.006	−0.527 ± 0.004
1c	−0.201 ± 0.005	−0.539 ± 0.007
1d	−0.151 ± 0.003	−0.516 ± 0.006
1e	−0.131 ± 0.003	−0.517 ± 0.007
1f	−0.058 ± 0.002	−0.510 ± 0.016

[a] $a_{X,1\text{-propanol}}$ is the first-order derivative of the logarithm of the observed rate constant in the presence of 1-propanol relative to that in water with respect to the molality of 1-propanol. [b] $a_{X,NMS}$ is the first-order derivative of the logarithm of the observed rate constant in the presence of NMS relative to water with respect to the molality of NMS (eqs 3 and 4).

The data in Table 3 are in good agreement with our previous findings,[31] showing that the rate-retarding effects of added 1-propanol are different for the different substituted probes. The rate-retarding effects of NMS are larger than those of 1-propanol and vary only slightly in the series **1a**−**f**. The rate-retarding effect of NMS on the hydrolysis of **1c** determined here is in good agreement with the $G(c)$ value for the same combination of hydrolytic probe and cosolute determined by Noordman et al.[67] In addition, we note that the work by Noordman et al.[67] also suggests that results rather similar to those reported here for NMS would have been obtained if sodium ethyl sulfate had been used as a headgroup mimic. The effects of NMS on the hydrolysis of **1a**−**f** are reminiscent of the effects of TMAB,[31] where the slopes $a_{X,TMAB}$, obtained by fitting $\ln(k_{X,TMAB}/k_{X,water})$ versus m_{TMAB}, were found to vary only slightly with the substituent. However, the values of $a_{X,NMS}$ are on average 2 times those of $a_{X,TMAB}$. Therefore, the hydrolysis of all of the probes is more retarded by added NMS than by added TMAB.

As in our previous work,[31] we assume that the micellar rate-retarding effect for each hydrolytic probe corresponds to the sum of the effects of the two mimicking compounds

$$\ln\left(\frac{k_{X,\,1\text{-propanol}}}{k_{X,\,water}}\right) + \ln\left(\frac{k_{X,\,NMS}}{k_{X,\,water}}\right) = \ln\left(\frac{k_{X,\,mic}}{k_{X,\,water}}\right) \tag{5}$$

By substituting eqs 3 and 4 into eq 5, we obtain

$$a_{X,\,1\text{-propanol}}m_{1\text{-propanol}} + a_{X,\,NMS}m_{NMS} = c_X \tag{6}$$

where c_X is the natural logarithm of the micellar rate constant relative to water. Equation 6 can be written for each substituted probe **1a**−**f** taking into account the different sensitivities of the different probes to added 1-propanol and NMS as quantified by $a_{X,NMS}$ and $a_{X,1\text{-propanol}}$.

Alternatively, $\ln(k_{X,mic}/k_{X,water})$ can be interpreted as the difference in activation Gibbs energy in water and in the micelle, or the equivalent difference in the Gibbs energy changes for binding to micelles of the reactant state and transition state (eq 7), with

Table 4. Molalities and Molar Concentrations[a] of 1-Propanol and NMS in Solution 1 and Solution 2

	mol kg^{-1}		mol dm^{-3}		
	1-propanol	NMS	1-propanol	NMS	water
solution 1	3.4 ± 0.2	4.5 ± 0.1	2.2 ± 0.1	2.88 ± 0.05	35.2 ± 0.3
solution 2	2.8 ± 0.2	5.5 ± 0.3	1.8 ± 0.1	3.5 ± 0.2	35.3 ± 0.8

[a] Molar concentrations were calculated using the experimentally determined densities of solution 1 and solution 2 at 25 °C (1.15 and 1.21 g cm^{-3}, respectively).

Table 5. Rate-Retarding Effects of 1-Propanol and NMS in Solution 1 on the Hydrolysis of Substituted Probes 1a−f at 25 °C

	$a_{X,1\text{-propanol}}m_{1\text{-propanol}}$[a,b]	$a_{X,NMS}m_{NMS}$[a,b]
1a	−0.81 ± 0.05	−2.48 ± 0.06
1b	−0.80 ± 0.05	−2.39 ± 0.04
1c	−0.69 ± 0.05	−2.45 ± 0.05
1d	−0.52 ± 0.03	−2.34 ± 0.05
1e	−0.45 ± 0.03	−2.35 ± 0.05
1f	−0.20 ± 0.01	−2.31 ± 0.08

[a] $a_{X,1\text{-propanol}}$ and $a_{X,NMS}$ are the first derivatives of the logarithms of the rate constants relative to those in water with respect to the molality of 1-propanol and NMS, respectively (Table 3). [b] $m_{1\text{-propanol}}$ and m_{NMS} have the values of the molalities of 1-propanol and NMS, respectively, in solution 1 (Table 4).

the caveat that the reactant state includes two molecules of water[31,32]

$$\ln\left(\frac{k_{X,mic}}{k_{X,water}}\right) = \frac{\Delta^{\ddagger}G^{\theta}_{X,water} - \Delta^{\ddagger}G^{\theta}_{X,mic}}{RT} = \frac{\Delta_{mic}G^{\theta}_{X}(R) - \Delta_{mic}G^{\theta}_{X}(AC)}{RT} \quad (7)$$

where $\Delta^{\ddagger}G^{\theta}_{X,water}$ and $\Delta^{\ddagger}G^{\theta}_{X,mic}$ are the standard molar activation Gibbs energies for the hydrolysis reaction in pure water and in the micellar pseudophase, respectively; $\Delta_{mic}G^{\theta}_{X}(R)$ and $\Delta_{mic}G^{\theta}_{X}(AC)$ are the standard molar Gibbs energy differences for binding to micelles of reactant (R) and activated complex (AC), respectively; and RT is the product of the gas constant and the absolute temperature. Equation 7 shows that the micellar rate-retarding effect exerted on the hydrolysis of each probe **1a**−**f** is caused by a more pronounced stabilization of the reactant state by binding to micelles in comparison with the stabilization of the transition state by binding to micelles.

Substitution of eq 7 into eq 6 leads to the equation

$$a_{X,1\text{-propanol}}m_{1\text{-propanol}} + a_{X,NMS}m_{NMS} = \frac{\Delta^{mic}G^{\theta}_{X}(R) - \Delta^{mic}G^{\theta}_{X}(AC)}{RT} \quad (8)$$

Equation 8 highlights that the difference between the stabilization of the initial state by binding to micelles and the stabilization of the transition state by binding to micelles is due to the combination of the effects exerted by surfactant tails, reproduced through $a_{X,1\text{-propanol}}m_{1\text{-propanol}}$, and by SDS headgroups, reproduced through $a_{X,NMS}m_{NMS}$.

The mimicking aqueous solution of the micellar pseudophase should be the same for all probes and therefore contains the two cosolutes in the same molalities, $m_{1\text{-propanol}}$ and m_{NMS}, for all probes **1a**−**f**. This is made explicit by rewriting the set of all eqs 6 in matrix form as

$$\begin{pmatrix} a_{MeO,\,1\text{-propanol}} & a_{MeO,\,NMS} \\ a_{Me,\,1\text{-propanol}} & a_{Me,\,NMS} \\ a_{H,\,1\text{-propanol}} & a_{H,\,NMS} \\ a_{Cl,\,1\text{-propanol}} & a_{Cl,\,NMS} \\ a_{F_3CO,\,1\text{-propanol}} & a_{F_3CO,\,NMS} \\ a_{NO_2,\,1\text{-propanol}} & a_{NO_2,\,NMS} \end{pmatrix} \begin{pmatrix} m_{1\text{-propanol}} \\ m_{NMS} \end{pmatrix} = \begin{pmatrix} c_{MeO} \\ c_{Me} \\ c_{H} \\ c_{Cl} \\ c_{F_3CO} \\ c_{NO_2} \end{pmatrix} \quad (9)$$

Equation 9 represents an overdetermined system that cannot be solved exactly. By applying singular value decomposition,[52] a solution we refer to as solution 1 in Table 4 was determined.

The required molalities for both 1-propanol and NMS are nonzero and (statistically) significant, showing that both 1-propanol and NMS are required to reproduce the observed micellar kinetics for **1a**−**f**. Based on the molalities of NMS and 1-propanol in solution 1 (Table 4) and the sensitivities of the rate constants for hydrolysis of the kinetic probes to the presence of NMS and 1-propanol (Table 3), the contributions of interactions with the surfactant tails and interactions with the surfactant headgroups to the overall observed rate retardation can be calculated (Table 5).

Table 5 shows that the product $a_{X,NMS}m_{NMS}$ is between 3 (**1a**) and 11 (**1f**) times larger than the product $a_{X,1\text{-propanol}}m_{1\text{-propanol}}$. Therefore, the micellar stabilization of the reactant state relative to the transition state for the hydrolysis reactions studied here is mainly due to ionic interactions of **1a**−**f** with SDS headgroups. However, although ionic interactions make the largest contribution to the observed rate-retarding effects, other properties of the Stern region of SDS such as those quantified by the $E_T(30)$ value and the Hammett ρ value for hydrolysis of **1a**−**f** cannot be reproduced by a solution of NMS alone and require the inclusion of 1-propanol (vide infra).

The hydrolysis of **1a**−**f** was studied in solution 1 to test whether solution 1 indeed reproduces experimentally the micellar rate effects exerted by SDS, as eq 9 predicts it should. As shown in Figure 3a and Table 6, solution 1 does not fully reproduce the rate-retarding effects exerted by the Stern region of SDS micelles.

Second Model Solution. To decrease the deviations in the experimentally observed rate effects for our model solution from the micellar rate effects, we improved the mathematical description leading to the model solution. The plots describing the kinetic effects of the two mimicking compounds on hydrolysis of **1a**−**f** (Figure 2a,b) start to deviate from linearity at high cosolute concentrations. This is particularly the case for added NMS at molalities above 3 mol kg^{-1}. The deviations suggest that higher-order interactions[65] (higher than pairwise) of cosolutes with reactants **1a**−**f** cannot be neglected for concentrated solutions of mimicking compounds.

As shown in Figure 2, the effects exerted by NMS (and, to some extent, by 1-propanol) are better reproduced using second-order polynomials instead of linear fits. This suggests that our model could be improved by the introduction of quadratic terms

in the mathematical description of the kinetic effects exerted by the model solutions. By adding quadratic terms to eq 6, one obtains

$$a'_{\mathrm{X,\,1\text{-}propanol}} m_{\mathrm{1\text{-}propanol}} + \frac{1}{2} b_{\mathrm{X,\,1\text{-}propanol}} m_{\mathrm{1\text{-}propanol}}{}^2 + a'_{\mathrm{X,\,NMS}} m_{\mathrm{NMS}} + \frac{1}{2} b_{\mathrm{X,\,NMS}} m_{\mathrm{NMS}}{}^2 = c_{\mathrm{X}} \quad (10)$$

Here, $a'_{\mathrm{X,1\text{-}propanol}}$ and $a'_{\mathrm{X,NMS}}$ have the same meaning as $a_{\mathrm{X,1\text{-}propanol}}$ and $a_{\mathrm{X,NMS}}$ in eq 6 (vide supra), but whereas $a_{\mathrm{X,1\text{-}propanol}}$ and $a_{\mathrm{X,NMS}}$ are determined from a linear fit, $a'_{\mathrm{X,1\text{-}propanol}}$ and $a'_{\mathrm{X,NMS}}$ are determined by a second-order polynomial fitting of the same experimental data (see Figure 2a,b for examples). Parameters $b_{\mathrm{X,1\text{-}propanol}}$ and $b_{\mathrm{X,NMS}}$ denote the second-order derivatives (hence the factor $^1/_2$) of the logarithms of the relative rate constants with respect to the molalities of 1-propanol and NMS, respectively. The mixed second-order derivative of the logarithms of the relative rate constants with respect to the molalities of 1-propanol and NMS is not included in eq 10 because this term is not accessible experimentally using separate solutions of 1-propanol and NMS. A mixed second-order derivative would describe 2:1 interactions between 1-propanol, NMS, and the kinetic probe. An evaluation of the mixed second-order derivative would require the experimental determination of the rate-retarding effects exerted on hydrolysis of **1a**−**f** for a series of solutions containing both 1-propanol and NMS. Our previous[31] method for accounting for the nonlinear rate-retarding effects at high molalities of 1-propanol and salt partially addressed the missing cross term, but at great experimental expense (vide infra).

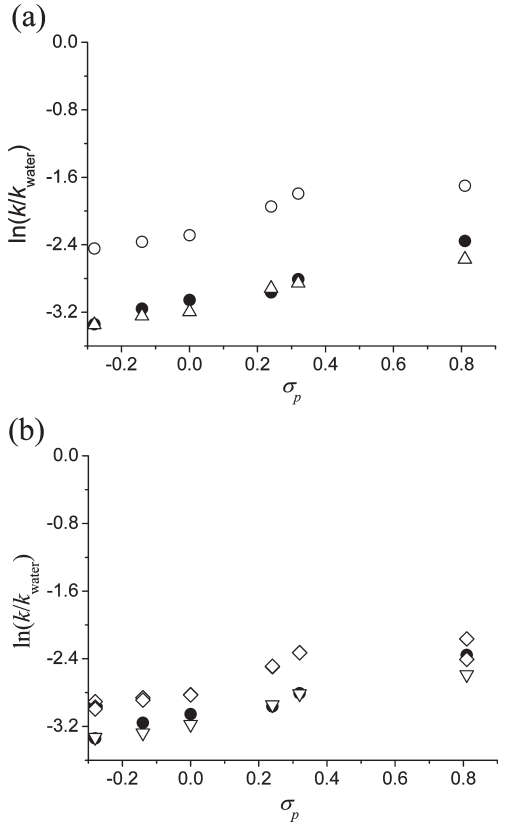

Figure 3. Rate-retarding effects of micelles (●) exerted on the hydrolysis of **1a**−**f** reproduced by the calculations underpinning our (a, Δ) first- and (b, ∇) second-order models and experimentally by the kinetic effects of (a, ○) solution 1 and (b, ◇) solution 2 on the hydrolysis of **1a**−**f**. The rate-retarding effects are plotted as a function of the Hammett substituent constants (σ_{p}).

The values of all derivatives $a'_{\mathrm{X,1\text{-}propanol}}$, $a'_{\mathrm{X,NMS}}$, $b_{\mathrm{X,1\text{-}propanol}}$, and $b_{\mathrm{X,NMS}}$ in eq 10 for different substituted hydrolytic probes are collected in Table 7.

As before, the system of eqs 10 can be written in matrix form as

$$\begin{pmatrix} a'_{\mathrm{MeO,\,1\text{-}propanol}} & \frac{1}{2} b_{\mathrm{MeO,\,1\text{-}propanol}} & a'_{\mathrm{MeO,\,NMS}} & \frac{1}{2} b_{\mathrm{MeO,\,NMS}} \\ a'_{\mathrm{Me,\,1\text{-}propanol}} & \frac{1}{2} b_{\mathrm{Me,\,1\text{-}propanol}} & a'_{\mathrm{Me,\,NMS}} & \frac{1}{2} b_{\mathrm{Me,\,NMS}} \\ a'_{\mathrm{H,\,1\text{-}propanol}} & \frac{1}{2} b_{\mathrm{H,\,1\text{-}propanol}} & a'_{\mathrm{H,\,NMS}} & \frac{1}{2} b_{\mathrm{H,\,NMS}} \\ a'_{\mathrm{Cl,\,1\text{-}propanol}} & \frac{1}{2} b_{\mathrm{Cl,\,1\text{-}propanol}} & a'_{\mathrm{Cl,\,NMS}} & \frac{1}{2} b_{\mathrm{Cl,\,NMS}} \\ a'_{\mathrm{F_3CO,\,1\text{-}propanol}} & \frac{1}{2} b_{\mathrm{F_3CO,\,1\text{-}propanol}} & a'_{\mathrm{F_3CO,\,NMS}} & \frac{1}{2} b_{\mathrm{F_3CO,\,NMS}} \\ a'_{\mathrm{NO_2,\,1\text{-}propanol}} & \frac{1}{2} b_{\mathrm{NO_2,\,1\text{-}propanol}} & a'_{\mathrm{NO_2,\,NMS}} & \frac{1}{2} b_{\mathrm{NO_2,\,NMS}} \end{pmatrix} \times \begin{pmatrix} m_{\mathrm{1\text{-}propanol}} \\ m_{\mathrm{1\text{-}propanol}}{}^2 \\ m_{\mathrm{NMS}} \\ m_{\mathrm{NMS}}{}^2 \end{pmatrix} = \begin{pmatrix} c_{\mathrm{MeO}} \\ c_{\mathrm{Me}} \\ c_{\mathrm{H}} \\ c_{\mathrm{Cl}} \\ c_{\mathrm{F_3CO}} \\ c_{\mathrm{NO_2}} \end{pmatrix} \quad (11)$$

Equation 11 cannot be solved using singular value decomposition. Solving eq 11 numerically using the Levenberg−Marquardt method[53] results in the solution referred to as solution 2 (Table 4). As for solution 1, the molalities of NMS and 1-propanol in solution 2 are nonzero and (statistically) significant, indicating that both components are essential in the micelle-mimicking solution. The individual rate-retarding effects of NMS and 1-propanol in solution 2 are calculated using the molalities of NMS and 1-propanol in solution 2 and the first and the second derivative for each of the two mimics. Table 8 lists these individual contributions.

Table 8 again shows that the largest part of the overall rate-retarding micellar effect is mimicked by NMS. Nevertheless,

Table 6. Kinetic Effects Exerted by Solution 1 and Solution 2 Relative to Those Exerted by SDS Micelles at 25 °C

	$k_{\mathrm{X,solution\ 1}}$ (10^{-4} s^{-1})	$k_{\mathrm{X,solution\ 2}}$ (10^{-4} s^{-1})	$\ln(k_{\mathrm{X,solution\ 1}}/k_{\mathrm{X,mic}})$	$\ln(k_{\mathrm{X,solution\ 2}}/k_{\mathrm{X,mic}})$
1a	0.356 ± 0.001	0.203 ± 0.003	0.89 ± 0.01	0.37 ± 0.02
1b	0.884 ± 0.006	0.531 ± 0.01	0.81 ± 0.05	0.31 ± 0.05
1c	2.155 ± 0.001	1.255 ± 0.004	0.65 ± 0.05	0.10 ± 0.05
1d	5.14 ± 0.01	2.98 ± 0.01	1.01 ± 0.01	0.47 ± 0.01
1e	7.17 ± 0.01	4.20 ± 0.01	1.01 ± 0.01	0.48 ± 0.01
1f	50.8 ± 0.5	28 ± 4	0.65 ± 0.08	0.06 ± 0.16

Table 7. Sensitivities of the Rate Constants for Hydrolysis of Probes 1a−f to 1-Propanol and NMS in Accordance with the Mathematical Description Leading to Solution 2

	$a'_{X,1\text{-propanol}}$ [a]	$a'_{X,NMS}$ [a]	$^1/_2 b_{X,1\text{-propanol}}$ [b]	$^1/_2 b_{X,NMS}$ [b]
1a	−0.212 ± 0.008	−0.58 ± 0.01	−0.007 ± 0.002	0.016 ± 0.003
1b	−0.213 ± 0.01	−0.555 ± 0.006	−0.005 ± 0.002	0.013 ± 0.001
1c	−0.187 ± 0.008	−0.571 ± 0.009	−0.004 ± 0.002	0.017 ± 0.002
1d	−0.149 ± 0.005	−0.549 ± 0.008	−0.0008 ± 0.001	0.016 ± 0.002
1e	−0.124 ± 0.006	−0.565 ± 0.01	−0.002 ± 0.001	0.022 ± 0.003
1f	−0.056 ± 0.004	−0.555 ± 0.02	−0.001 ± 0.001	0.021 ± 0.005

[a] $a'_{X,1\text{-propanol}}$ and $a'_{X,NMS}$ are the first-order derivatives of the logarithms of the rate constants relative to those in water with respect to the molalities of 1-propanol and NMS, respectively (eqs 10 and 11). [b] $b_{X,1\text{-propanol}}$ and $b_{X,NMS}$ are the second-order derivatives of the logarithms of the rate constants relative to water with respect to the molalities of 1-propanol and NMS, respectively (eqs 10 and 11).

Table 8. Rate-Retarding Effects of 1-Propanol and NMS in Solution 2 on the Hydrolysis of Probes 1a−f at 25 °C

probe	$a'_{X,1\text{-propanol}} m_{1\text{-propanol}} + {}^1/_2 b_{X,1\text{-propanol}} (m_{1\text{-propanol}})^{2}$ [a,b]	$a'_{X,NMS} m_{NMS} + {}^1/_2 b_{X,NMS} (m_{NMS})^{2}$ [b,c]
1a	−0.64 ± 0.06	−2.69 ± 0.17
1b	−0.63 ± 0.07	−2.65 ± 0.09
1c	−0.55 ± 0.06	−2.63 ± 0.13
1d	−0.42 ± 0.04	−2.52 ± 0.12
1e	−0.36 ± 0.04	−2.45 ± 0.16
1f	−0.17 ± 0.02	−2.42 ± 0.26

[a] $a'_{X,1\text{-propanol}}$ and $b_{X,1\text{-propanol}}$ are the first- and second-order derivatives, respectively, of the logarithms of the rate constants relative to water with respect to the molality of 1-propanol (Table 7). [b] $m_{1\text{-propanol}}$ and m_{NMS} are the molalities of 1-propanol and NMS, respectively, in solution 2 (Table 4). [c] $a'_{X,NMS}$ and $b_{X,NMS}$ are the first- and second-order derivatives, respectively, of the logarithms of the rate constants relative to water with respect to the molality of NMS (Table 7).

although the contributions to the overall rate-retarding effect that are mimicked by 1-propanol are relatively small, they vary rather strongly between the hydrolytic probes. This variation in rate-retarding effects between hydrolytic probes results in the difference in the Hammett ρ values between reaction in bulk water and in the micellar pseudophase. Consequently, this change in Hammett ρ value cannot be accounted for without the inclusion of 1-propanol in the model solutions, which, in turn, explains why the calculated molalities of 1-propanol and NMS in the mimicking solutions are both nonzero and statistically significant.

The hydrolysis-rate-retarding effects experienced by **1a**−**f** in solution 2 were determined experimentally and compared to the kinetic effects exerted by micelles and to the kinetic effects of solution 1. Figure 3a,b and Table 6 show that, for all substituted probes **1a**−**f**, the rate-retarding effects of SDS micelles are experimentally reproduced considerably better by solution 2 than by solution 1.

The fact that solution 2 reproduces the micellar data better than solution 1 shows the merit of including both 1:1 and 2:1 interactions over extrapolating the 1:1 interactions from relatively dilute aqueous solutions of the cosolutes into the more concentrated regimes. Although solution 2 is better, it still does not retard the hydrolysis of **1a**−**f** to exactly the same extent as SDS micelles, with rate constants overestimated by up to a factor of 1.6. Nevertheless, this indicates that at least 83% of the change in $\Delta^{\ddagger}G^{\theta}$ has been accounted for. The remaining deviations between the rate-retarding effects exerted by solution 2 and the corresponding rate-retarding effects exerted by the Stern region of SDS micelles are attributed to the lack of terms describing the cross interactions between the two mimicking compounds in eqs 10 and 11, that is the mixed derivatives (vide supra).

Previously,[31] we derived a second-generation model solution for CTAB micelles by taking the first model solution as a reference and determining correction terms for the molalities of 1-propanol and tetramethylammonium bromide (TMAB) in solution 1 using singular value decomposition. This method of deriving solution 2 required the experimental determination of the rate-retarding effects exerted on hydrolysis of **1a**−**f** in solutions containing both 1-propanol and TMAB in high molalities, namely around the molalities in solution 1. Our present improved mathematical description leading to solution 2 represents a faster method of directly deriving the second model solution because it does not require additional experimental data.

To test the generality of the results obtained with the kinetic probes, another type of probe, namely the solvatochromic $E_T(30)$ probe, was used in an experiment to assess the predictive value of our model solutions for processes unrelated to those used to develop the model solutions themselves. The $E_T(30)$ probe is considered one of the most useful indicators for the polarity of its environment.[68,69] In aqueous micelle solutions, the solvatochromic probe binds to the micellar Stern region,[38,70] and for micelles formed by cationic surfactants such as cetyltrimetylammonium chloride and dodecyltrimetylammonium chloride, the $E_T(30)$ value was found to vary with surfactant concentration.[40] For anionic SDS, the position of the longest-wavelength absorbance band of a solvatochromic merocyanine dye analogous to the $E_T(30)$ dye has been reported[41] to be virtually constant with SDS concentration in the range of 0.016−0.204 mol dm^{-3}. To confirm that the $E_T(30)$ value does not change with SDS concentration above the cmc, we determined the $E_T(30)$ value for solutions in the range of 0.01−0.1 mol dm^{-3} SDS. The position of the longest-wavelength absorbance band was found to be practically constant, namely 498.4 ± 0.5 nm, corresponding to an $E_T(30)$ value of 57.4 kcal mol^{-1}. The $E_T(30)$ value of 57.4 kcal mol^{-1} is in good agreement with the value of 57.5 kcal mol^{-1} reported in the literature.[70]

The $E_T(30)$ value for solution 2 equals the $E_T(30)$ value of 57.4 kcal mol^{-1} for the SDS micellar medium, whereas the $E_T(30)$ value for solution 1 is 57.0 kcal mol^{-1}. Hence, as reported by the solvatochromic dye, the micropolarity of solution 2 is identical to that of the Stern region of SDS micelles. To confirm that this is a significant result, the $E_T(30)$ values for aqueous solutions of different concentrations of NMS and 1-propanol, in the ranges of 2.5−6.5 mol kg^{-1} for NMS and 2.0−3.5 mol kg^{-1} for 1-propanol (i.e. around the molalities in solution 2) were determined. This experiment probes the sensitivity of the solvatochromic probe to changes in concentration of the two mimicking compounds. As shown in the Supporting Information (Figure S6.1), the $E_T(30)$ value is not very sensitive to changes in the molality of NMS and is almost completely determined by the molality of 1-propanol, in line with an earlier report[71] showing that highly polar solutes have only a small effect on the polarity of aqueous solutions. These relative sensitivities are the exact

opposite of the relative sensitivities of our hydrolytic probe reactions. According to the solvatochromic probe, solution 2 fully reproduces the polarity of the micellar interfacial region, whereas the polarity of solution 1 is close to that of SDS micelle interface. The result obtained with the $E_T(30)$ probe confirms the outcome of our kinetic analysis, namely solution 2 reproduces the interfacial region of SDS micelles better than solution 1. Because the solvatochromic probe was not used in the construction of the model solutions, the identical $E_T(30)$ value for solution 2 and the micellar pseudophase demonstrates that solution 2 can be used to predict medium-controlled properties of the Stern region of SDS micelles that were not included in our modeling. The fact that solution 2 accurately reproduces the polarity of the Stern region as reported by the $E_T(30)$ probe, despite the relative sensitivities of the $E_T(30)$ probe to 1-propanol and NMS being the exact opposite of the sensitivities of our hydrolytic probes, confirms that both 1-propanol and NMS are required to reproduce the properties of the micellar Stern region studied here.

In our kinetic study of the SDS micellar pseudophase, the linear alkyl group of 1-propanol mimics the surfactant backfolding tail in the micellar Stern region. However, the hydroxyl in 1-propanol is not representative of the hydrocarbon tail of the surfactant and, in fact, more closely resembles water. In that sense, 1-propanol in solution 2 also reproduces a small fraction of water in the SDS micellar pseudophase. In line with this fact, product analysis using HPLC (Supporting Information, section S7) revealed that some ester formation occurs in addition to hydrolysis in solution 2. Further detailed product analysis at various water/1-propanol ratios shows that, in these mixtures, the reactivity of 1-propanol, leading to ester formation, is twice the reactivity of water, leading to hydrolysis (Supporting Information, section S8). Because the reactivity of the hydroxyl in 1-propanol is similar to that of water, we define the "effective water concentration" in solution 2, $[H_2O]_{effective}$, as

$$[H_2O]_{effective} \approx [H_2O]_{real} + [1\text{-propanol}] \quad (12)$$

(For a derivation and explanation of the apparent disappearance of a factor of 2, see section S8 in the Supporting Information.) Here, $[H_2O]_{real}$ is the real concentration of water, and [1-propanol] is the concentration of 1-propanol in solution 2. Equation 12 accounts for the (small) rate effect exerted by the reactivity of the hydroxyl functional group in 1-propanol, which does not represent polarity and hydrophobic effects as exerted by the hydrophobic tails of the surfactants (vide infra). Equation 12 gives an effective concentration of water in solution 2 of 37.0 mol dm^{-3}, suggesting that the water concentration in the interfacial region of SDS micelles is 37.0 mol dm^{-3}.

Factors Determining the Deceleration of the Hydrolysis of 1a−f by SDS Micelles. The relative micellar rate constant $k_{X,mic}/k_{X,water}$ is not constant for all probes **1a**−**f** and lies in the range of 0.03−0.09 (Table 2). A potential source for the differences in the rate-retarding effects exerted by SDS micelles on the different probes could, in principle, be solubilization in different locations in the SDS micellar pseudophase for different hydrolytic probes. However, we have previously[31] shown that all of the kinetic probes bind in the micellar Stern region, in line with findings by other authors for a wide range of molecules, such as benzophenone; butyronitrile; primary alcohols; solvatochromic indicators such as *p*-nitroanisol, *p*-nitroaniline, and the $E_T(30)$ probe;[34,35,72] and even benzene up to a critical concentration.[73,74] In addition, if one assumes that K_{mic} primarily represents the hydrophobicity of the hydrolytic probe and if more hydrophobic probes are expected to bind more, or deeper, in the hydrophobic micellar core, then an increase in K_{mic} (Table 1) should correspond to a decrease in the relative rate constant $k_{X,mic}/k_{X,water}$ (Table 2). The fact that we did not find such a correlation suggests that differential binding sites are not an important factor behind the differences in rate-retarding effects. We therefore assume that, in line with the above-mentioned literature reports, all of the substituted probes bind in the same zone in the Stern region.

As in the case of the deceleration of the hydrolysis of **1a**−**f** by micelles of CTAB and DTAB, the rate-retarding effects exerted by micelles of SDS on the hydrolysis of **1a**−**f** are due to the particular features of the micellar pseudophase as a local reaction medium in comparison with the reaction environment as offered by bulk water. The main factors affecting the reactivity in the SDS micellar pseudophase are (1) the lower local concentration/activity of water, (2) the lower polarity and direct hydrophobic interactions with the surfactant tails, (3) the high ionic strength and direct interactions with the headgroups, and (4) the local charge in the Stern region. We now evaluate these factors.

The concentration of water (factor 1) in the second model solution is 35.3 mol dm^{-3} (Table 4). This represents a lower estimate of the water concentration in the micellar Stern region (vide supra), and a better estimate is 37.0 mol dm^{-3}. The hydrolysis of **1a**−**f** is second-order in water (Scheme 1). To estimate the kinetic effect of the lower local concentration of water, we express the pseudo-first-order rate constants for hydrolysis of **1a**−**f** in water, $k_{X,water}$, and in the micellar pseudophase, $k_{X,mic}$, as functions of the water concentrations in bulk water, $[H_2O]_{bulk}$, and in the micellar Stern region, $[H_2O]_{mic}$

$$k_{X,water} = k'_{X,water}[H_2O]_{bulk}^{\ 2} \quad (13)$$

$$k_{X,mic} = k'_{X,mic}[H_2O]_{mic}^{\ 2} \quad (14)$$

where $k'_{X,water}$ and $k'_{X,mic}$ are the third-order rate constants for hydrolysis in bulk water and in the micellar Stern region, respectively. Using the effective water concentration in solution 2 of 37.0 mol dm^{-3} gives a squared ratio $([H_2O]_{mic}/[H_2O]_{bulk})^2$ of 0.44. The lower concentration of water in the micellar pseudophase (factor 1) therefore accounts for only a ca. 2-fold decrease in the pseudo-first-order rate constants for hydrolysis of **1a**−**f**. Because $k_{X,mic}$ is on average 18-fold lower than $k_{X,water}$, the decreased water concentration explains only 12% of the rate-decreasing effect of hydrolysis exerted by SDS micelles.

Possibly a better way to account for the effects related to water reactivity is through its activity (factor 1). A high ionic strength, as well as added alcohols, leads to a decrease in the activity of water, but the extent of this decrease depends on the nature of the solutes.[75] Solution 2 has an ionic strength of 3.5 mol dm^{-3} (vide infra) and contains a high concentration of 1-propanol, suggesting that the activity of water in this solution is likely lower than that in bulk water. The individual effects exerted on the water activity by these two factors (i.e. the ionic strength and the concentration of 1-propanol) overlap and cannot be separated. The decrease in the activity of water could be fully due to the decrease in water concentration or could be caused by a combination of a decrease in the concentration of water and a decrease in the activity coefficient of water. To determine whether the activity coefficient of water in solution 2 differs from that in pure water, it is necessary to know the interfacial water activity relative to the activity of pure water. As found by Angeli et al.,[76]

using the pseudophase formalism for the experimentally observed equilibrium of hydration of *p*-alkyloxy-α-α-α-trifluoroacetophenone, the water activity in the interfacial region of SDS micelles relative to the activity of pure water equals 0.6. The value of 0.6 coincides with the value of the effective concentration of water in solution 2 relative to the concentration of water in pure water. On the basis of the results of Angeli et al.,[76] the activity coefficient of water in solution 2 equals the activity coefficient of bulk water. Therefore, the activity coefficient of water does not appear to contribute to the lower activity of water in the micellar pseudophase. This conclusion is in line with the observation by Rispens et al.[77] that "variations in the water reactivity ... hardly play a role in the observed medium effects [on the hydrolysis of an activated ester]." Similarly, Bunton et al.[78] and De Albrizzio and Cordes[79] found the water reactivity in the Stern region of SDS to be very similar to the water reactivity in bulk water. In summary, although the local concentration of water in the micellar Stern region of SDS is lower than that in bulk water and the activity coefficient of water might be lower than unity, the resulting overall rate-retarding effect on the hydrolysis of **1a**−**f** is unlikely to exceed a factor of 2.

With respect to the lower polarity of the micellar Stern region (factor 2), we note that polarity probes show that typical model solutions for the micellar pseudophase (i.e., binary mixtures such as *n*-alcohol/water, 1,4-dioxane/water, acetonitrile/water) are less polar than bulk water.[40,70,80] The $E_T(30)$ value for pure water is 63.1 kcal/mol,[68] whereas for solution 2, the $E_T(30)$ value is 57.4 kcal/mol; that is, the $E_T(30)$ probe reports a decrease in the polarity on going from bulk water to our second model solution. The $E_T(30)$ value is more sensitive to the change in concentration of 1-propanol than to the change in concentration of NMS (vide supra). In addition the $E_T(30)$ value for 4.2 mol dm^{-3} NMS, which is above the NMS concentration in solution 2, of 62.6 kcal/mol[32] is close to the $E_T(30)$ value of pure water (63.1 kcal/mol).[68] Because NMS does not contribute significantly to the decreased polarity of solution 2 compared to bulk water, the kinetic effects of the lower polarity of solution 2 on **1a**−**f** hydrolysis are dominated by the effect of 1.8 mol dm^{-3} 1-propanol. The lower polarity of the micellar pseudophase compared to the polarity of pure water contributes to the decrease in the rate of hydrolysis reactions in the presence of micelles.[45,81] The usual interpretation of this observation involves the higher polarity of the transition states (Scheme 1) compared to the polarity of the substituted substrates: a less polar medium is less favorable for hydrolysis. Therefore, the lower polarity of the Stern region of SDS micelles is responsible for part of the rate-retarding effects on the hydrolysis of **1a**−**f**. In addition to its effect on the local polarity, 1-propanol also engages in direct hydrophobic interactions with the probes used here, as well as with related hydrolytic probes, retarding hydrolysis.[66,82−85] Because added 1-propanol contributes to rate retardation through hydrophobic interactions with the hydrolytic probe and through the decrease in local polarity, these two effects cannot be separated. Nevertheless, it is of interest (vide infra) that the rate-retarding effect of 1-propanol varies between different hydrolytic probes, indicating that different reactions display different sensitivities to hydrophobic interactions, giving rise to changes in the Hammett ρ value for hydrolysis of **1a**−**f**. The effects of interactions with the hydrophobic surfactant tails of SDS, be they through direct hydrophobic interactions or through decreased local polarity, thus depend on the sensitivity of the reaction kinetics to such interactions, but in general, they can be modeled through 1.8 mol dm^{-3} 1-propanol. It should be noted that, although headgroup effects dominate the rate-retarding effect exerted by SDS micelles (vide infra), the increased Hammett ρ value for hydrolysis of **1a**−**f** in SDS micelles is the result of hydrophobic interactions and decreased local polarity, with negligible contribution from headgroup effects.

In addition to the local polarity and hydrophobic interactions, another factor to consider is the high ionic strength and direct interactions with the ionic groups in the Stern region of ionic micelles (factor 3).[45,86] In our model, the effects of ionic strength and direct ionic interactions are modeled by NMS. As argued above, the rate-retarding effects exerted in solution 2 by NMS on hydrolysis of probes **1a**−**f** cannot be attributed to a contribution of NMS to the decrease in polarity. Table 8 shows that the deceleration due to NMS in solution 2 represents at least 81% of the total rate-retarding effect exerted by solution 2 for all probes.

Differences in the stabilization of the reactant state and the activated complex by specific interactions with NMS could also influence the reactivity of probes **1a**−**f** in hydrolysis. To understand whether specific interactions with NMS contribute to the retardation of the rates of hydrolysis of **1a**−**f**, we compared the kinetic effects exerted by NMS with those exerted by other salts. If the kinetic effects do not depend on the nature of the salt, then the decelerating effects (Figure 2b) exerted by NMS on hydrolysis of **1a**−**f**, as quantified by the slopes of $\ln(k_{X,NMS}/k_{X,water})$ versus NMS molality, should be the same as the rate-retarding effects exerted by tetramethylammonium bromide (TMAB) on the hydrolysis of **1a**−**f** or the rate-retarding effect of NaCl on **1c**, for example. However, the slopes describing the sensitivities of the rates of hydrolysis to NMS ($a_{X,NMS}$ in Table 3) are higher by a factor of about 2 compared to the slopes representing the sensitivities of the hydrolysis rates to TMAB (Table 4 in ref 31). Therefore the rates of hydrolysis of **1a**−**f** are more retarded by NMS than by TMAB. Similarly, the rate-retarding effect of NaCl on the hydrolysis of **1c** as quantified through the pairwise interaction parameter $G^P(S)$ by Noordman et al.[87] corresponds to a slope of $\ln(k_{X,NaCl}/k_{X,water})$ versus NaCl molality of −0.25. We therefore conclude that the large rate-retarding effects exerted by NMS in solution 2 on the hydrolysis of **1a**−**f** result from the combination of the kinetic effects due to the high ionic strength with effects caused by specific interactions of **1a**−**f** with NMS. For the micellar solutions, this indicates that the combined effects of high local ionic strength and direct interactions between the sulfate headgroups of SDS and hydrolytic probes **1a**−**f** dominate the observed rate-retarding effects and that the effects of ionic strength and specific ionic interactions can be modeled through 3.5 mol dm^{-3} NMS. Nevertheless, although the effects of ionic strength and specific ionic interactions might dominate the observed rate-retarding effects, 1-propanol is still required in an effective micelle-mimicking solution to account for local polarity and hydrophobic interaction effects (vide supra).

The local negative charge in the Stern region of anionic SDS micelles (factor 4) has a destabilizing effect on the partial negative charge developing in the activated complex (Scheme 1). The local positive charge in the interfacial region of cationic micelles of CTAB and DTAB has the opposite effect, stabilizing the activated complex.[31] The combined effect of the electrostatic non-neutrality in the micellar interfacial region on the transition state[13,61,62] and specific interactions with surfactant headgroups explains why the micellar rate constants for SDS micelles (Table 1) are smaller by a factor of ca. 2.5 than those for CTAB and DTAB micelles.[31] The effect of the

non-neutrality of the micellar Stern region and the effect of specific interactions with the surfactant headgroups are not necessary orthogonal. We therefore make no attempt to separate the individual contributions. We note, however, that our model solution generally reproduces micellar kinetics well, despite the fact that it can obviously not be overall negatively charged. This suggests that a significant part of the rate-retarding effect of the electrostatic non-neutrality of the micellar Stern region is reproduced through direct interactions between the hydrolytic probes and negatively charged methyl sulfate. The implication of this conclusion for the micellar Stern region is that the local charge as a medium effect per se on the hydrolysis of **1a**−**f** might be of less importance than more specific interactions with the negatively charged headgroups themselves.

Comparison of the Description of the Stern Region of SDS Micelles by Model Solutions 1 and 2 with Previous Representations. The concentrations of NMS in the model solutions (2.9 mol dm^{-3} in solution 1 and 3.5 mol dm^{-3} in solution 2) provide estimates of the concentration of surfactant headgroups in the Stern region of SDS micelles. Both estimates are between our previously estimated limits of 2.5−5.4 mol dm^{-3}, calculated by considering the Stern region of SDS micelles as a layer between two concentric spheres.[6]

According to solution 2, the effective concentration of water in the Stern region of SDS micelles is 37.0 mol dm^{-3}. This value is in agreement with the interfacial water concentration at the average solubilization site of merocyanine dye $BuQMBr_2$ in SDS micelles of 38.9 mol dm^{-3}, as determined by Martins et al.[41] by comparison of the $E_T(BuQMBr_2)$ values for SDS micelles with a plot of $E_T(BuQMBr_2)$ versus concentration of water in solutions of 1-propanol. The ratio between the NMS and water concentrations of 10.6 is in reasonable agreement with a hydration number per surfactant of 8−9, as determined by Bales et al.[88] for SDS micelles with an aggregation number of approximately 63.

An important merit of the present model solutions over the simple salt solutions and aqueous alcohol solutions used previously for mimicking the Stern region of SDS micelles[32,45] is that solution 1 and solution 2 have the ability to reproduce both ionic and hydrophobic interactions experienced by a probe bound in the micellar interfacial region. The importance of using both headgroup and tail mimics is illustrated by the observation that the significant rate retardations can be accounted for only on the basis of interactions with the surfactant headgroups, as modeled by NMS, whereas the change in Hammett ρ value can be accounted for only through the lower local polarity and hydrophobic interactions with the surfactant tails, as mimicked by 1-propanol. Similarly, the inclusion of 1-propanol in the model solution allowed us to correctly predict the micellar $E_T(30)$ value, which we were unable to do using a concentrated salt solution alone.[32]

In both model solutions, the molality of NMS is higher than the molality of 1-propanol (Table 4). Additionally, for all probes **1a**−**f**, the sensitivity to NMS is larger than the sensitivity to 1-propanol ($a_{X,NMS}$ is at least 2 times $a_{X,1\text{-propanol}}$; Table 3). Consequently, the rate-retarding effects exerted on the hydrolysis of **1a**−**f** by SDS headgroups as mimicked by NMS ($a_{X,NMS}m_{NMS}$) are larger than the effects exerted by the surfactant tails as mimicked by 1-propanol ($a_{X,1\text{-propanol}}m_{1\text{-propanol}}$) (Table 5). The sum of the effects exerted by micellar headgroups and surfactant tails dictates the magnitude of the difference between the stabilization of the reactant state by binding to micelles and the stabilization of the transition state by binding to micelles (eq 8). However, different probes can have different sensitivities

Table 9. Molalities and Molar Concentrations[a] of 1-Propanol and Salt[b] in Solution 1 for SDS, DTAB, and CTAB Micelles

	mol kg^{-1}		mol dm^{-3}		
	1-propanol	salt[b]	1-propanol	salt[b]	water
SDS	3.4 ± 0.2	4.5 ± 0.1	2.2 ± 0.1	2.88 ± 0.05	35.2 ± 0.3
DTAB	9.3 ± 0.9	1.5 ± 0.6	5.1 ± 0.6	0.8 ± 0.3	30 ± 1.8
CTAB	5.0 ± 0.5	4.9 ± 0.3	2.6 ± 0.3	2.6 ± 0.2	29 ± 0.8

[a] Molar concentrations were calculated using the experimentally determined densities at 25 °C of the first model solutions for SDS, DTAB, and CTAB micelles (1.15, 0.97, and 1.08 g cm^{-3}, respectively). [b] NMS for SDS and tetramethylammonium bromide (TMAB) for DTAB and CTAB.

to interactions with surfactant headgroups and hydrocarbon tails that are reflected in the relative contributions of the two terms $a_{X,NMS}m_{NMS}$ and $a_{X,1\text{-propanol}}m_{1\text{-propanol}}$. For example, the relative effects of the two mimics are different in the case of the $E_T(30)$ probe, which is more sensitive to 1-propanol than to NMS. The effects exerted by 1-propanol and NMS on the value of the wavelength at the maximum of absorbance in the visible range (λ_{max}) of the $E_T(30)$ probe are estimated as $am_{1\text{-propanol}}$ and bm_{NMS} (section S2 in Supporting Information), which are (27.1 ± 3.2) nm and (−1.1 ± 1.6) nm, respectively. These values clearly show that the effects of the micellar Stern region on the $E_T(30)$ solvatochromic probe are dominated by polarity and hydrophobic effects as mimicked by 1-propanol. The fact that the hydrolysis of phenyl chloroformate is much less retarded by 4.3 mol dm^{-3} NMS than by SDS micelles represents another example.[45] As for the $E_T(30)$ probe, phenyl chloroformate (PhOCOCl) hydrolysis is probably more sensitive to interactions with the surfactant tails than to interactions with SDS headgroups; that is, in terms of eq 8, $a_{PhOCOCl,1\text{-propanol}}m_{1\text{-propanol}}$ is larger than $a_{PhOCOCl,NMS}m_{NMS}$. These two examples clearly illustrate the importance of modeling both hydrophobic and ionic interactions when developing universal model solutions for the micellar pseudophase.

Comparison of SDS Micelles with DTAB and CTAB Micelles in Terms of the Model Solution for the Stern Region. Analogous to our previous studies of cationic micelles of DTAB and CTAB,[31] we reproduce the Stern region of SDS micelles by a model solution containing a mimic of the headgroup (NMS) and a mimic of the backfolding surfactant tail (1-propanol). Applying our previous mathematical description, based on first-order derivatives, that led to the model solutions for micelles of DTAB and CTAB, we found the first model solution for SDS micelles.

Comparison of the concentrations of salt and 1-propanol in the first model solutions for SDS, DTAB, and CTAB micelles (Table 9) shows that the local concentration of the backfolding surfactant tails in the case of SDS micelles more closely resembles the corresponding concentration for CTAB micelles than the respective concentration for DTAB micelles. In addition, the micellar binding constants (K_m) for **1a**−**f** binding to SDS are closer to the corresponding K_m values for CTAB, but ca. 3 times larger than the micellar binding constants for DTAB.[31] Our results therefore suggest that the interfacial region of SDS micelles is structurally more similar to the Stern region of CTAB micelles than to the Stern region of DTAB micelles.

The molalities of 1-propanol and TMAB in solution 2 for CTAB micelles are 7.7 and 5.7 mol kg^{-1}, respectively.[31] The density of this solution was determined to be 1.04 g dm^{-3}, allowing

the calculation of the molar concentrations of 1-propanol and TMAB in solution 2 for CTAB micelles as 3.4 and 2.5 mol dm^{-3}, respectively. Therefore, the second-order solutions for SDS micelles (Table 4) and CTAB micelles are less similar to each other than are the first-order solutions for SDS micelles and CTAB micelles (Table 9). Comparison of the concentrations of 1-propanol in the model solutions for SDS and CTAB suggests that backfolding surfactant tails have a greater effect on the local reaction medium in CTAB than in SDS. The opposite is the case for the effect of the ionic headgroups.

CONCLUSIONS

The Stern region of SDS micelles has been modeled by concentrated solutions of surfactant headgroup mimic NMS and surfactant tail mimic 1-propanol. A first model solution (solution 1) was derived by singular value decomposition of extrapolated linear fits of experimental rate-retarding effects of NMS and 1-propanol on a series of hydrolytic probes. Solution 1 reproduces approximately one-half of the experimentally observed micellar rate retardations for the hydrolytic probes. We attribute this discrepancy to the fact that nonlinear contributions to the rate-retarding effects of NMS and 1-propanol cannot be neglected at high concentrations. We therefore improved our mathematical approach to the deconvolution of micellar effects by incorporating quadratic terms in the equations reproducing the rate-retarding effects of the mimicking compounds and incorporating the terms in our matrix equation. Numerically solving the system of nonlinear equations thus obtained, we determined a second model solution (solution 2) that reproduces the rate-retarding effects of SDS micelles to within a factor of 1.6. Solution 2 also correctly predicts the micropolarity of SDS micelles as reported by the solvatochromic $E_T(30)$ probe. The second model solution can therefore be used to estimate rate constants for reactions occurring at the surface of SDS micelles and similar medium-sensitive properties, when a direct determination of these is not possible.

In addition to predicting medium effects on reactions, our approach also allows the dissection of the overall medium effect into contributions originating from surfactant headgroups and surfactant tails, that is from ionic and hydrophobic interactions. For the hydrolysis of **1a**−**f**, we showed that the water activity and the local charge are not important contributors to the rate-retarding effects. The dominant rate-retarding effects result from the combination of high ionic strength and direct interactions with the surfactant headgroups as modeled by NMS. The combination of hydrophobic interactions and the decreased local polarity as modeled by 1-propanol also make a contribution to rate retardation, but the importance of these is more obvious in that they are required to explain the increased Hammett ρ in the micellar pseudophase, as well as the micellar $E_T(30)$ value. The combination of these observations, that is significantly decreased rate constants for hydrolysis and increased Hammett ρ value, can only be reproduced using our model solution containing *both* headgroup *and* tail mimics. We anticipate that the ability to separate the different contributions allows the design of alternative surfactants with tailored properties for a variety of reactions.

Our current results for anionic SDS micelles, in combination with our previous results for cationic micelles of DTAB and CTAB, suggest that our approach is generally valid for micelle-forming surfactants and probably for vesicle-forming surfactants as well.

ASSOCIATED CONTENT

Supporting Information. Kinetic effects of SDS micelles on hydrolysis of **1d** at different values of bulk pH; rate constants of hydrolysis for **1a**−**f** in aqueous solutions of SDS; Hammett plots for hydrolysis of **1a**−**f** in water and in the Stern regions of SDS, CTAB, and DTAB micelles; rate constants of hydrolysis for **1a**−**f** in aqueous solutions of sodium methylsulfate and 1-propanol; sensitivity of the solvatochomic $E_T(30)$ probe to molality of added 1-propanol and NMS; HPLC analyses of reaction products; and rate constants of hydrolysis and esterification and calculation of the effective water concentration. This material is available free of charge via the Internet at http://pubs.acs.org.

AUTHOR INFORMATION

Corresponding Author

*Tel.: +44 (0)29 208 70301. Fax: +44 (0)29 208 74030. E-mail: buurma@cardiff.ac.uk.

ACKNOWLEDGMENT

We thank EPSRC for funding (EP/D001641/1) and the POC Centre research groups at Cardiff University for useful discussions.

REFERENCES

(1) Israelachvili, J. N.; Mitchell, D. J.; Ninham, B. W. *J. Chem. Soc., Faraday Trans. 2* **1976**, *72*, 1525–1568.
(2) Gruen, D. W. R. *Prog. Colloid Polym. Sci.* **1985**, *70*, 6–16.
(3) Clemett, C. J. *J. Chem. Soc. A: Inorg., Phys., Theor. Chem.* **1970**, 2251–2254.
(4) Bocker, J.; Brickmann, J.; Bopp, P. *J. Phys. Chem.* **1994**, *98*, 712–717.
(5) Menger, F. M.; Portnoy, C. E. *J. Am. Chem. Soc.* **1967**, *89*, 4698–4703.
(6) Buurma, N. J. *Adv. Phys. Org. Chem.* **2009**, *43*, 1–37.
(7) Dwars, T.; Paetzold, E.; Oehme, G. *Angew. Chem., Int. Ed.* **2005**, *44*, 7174–7199.
(8) Taşcioglu, S. *Tetrahedron* **1996**, *52*, 11113–11152.
(9) Li, C. J.; Chen, L. *Chem. Soc. Rev.* **2006**, *35*, 68–82.
(10) Iglesias, E. *J. Phys. Chem. B* **2001**, *105*, 10287–10294.
(11) Khan, M. N. *Micellar Catalysis*; CRC Press: Boca Raton, FL, 2007.
(12) Bunton, C. A. *Adv. Colloid Interface Sci.* **2006**, *123*−*126*, 333–343.
(13) Campos-Rey, P.; Cabaleiro-Lago, C.; Hervés, P. *J. Phys. Chem. B* **2010**, *114*, 14004–14011.
(14) Onel, L.; Buurma, N. J. *Annu. Rep. Prog. Chem. B: Org. Chem.* **2009**, *105*, 363–379.
(15) Onel, L.; Buurma, N. J. *Annu. Rep. Prog. Chem. B: Org. Chem.* **2010**, *106*, 344–375.
(16) Buurma, N. J. *Annu. Rep. Prog. Chem. B: Org. Chem.* **2011**, *107*, 328–348.
(17) Marin, M. A. B.; Nome, F.; Zanette, D.; Zucco, C.; Romsted, L. S. *J. Phys. Chem.* **1995**, *99*, 14572.
(18) Krasovskiy, A.; Duplais, C.; Lipshutz, B. H. *J. Am. Chem. Soc.* **2009**, *131*, 15592–15593.
(19) Lipshutz, B. H.; Chung, D. W.; Rich, B. *Org. Lett.* **2008**, *10*, 3793–3796.
(20) Lipshutz, B. H.; Ghorai, S.; Aguinaldo, G. T. *Adv. Synth. Catal.* **2008**, *350*, 953–956.
(21) Lipshutz, B. H.; Petersen, T. B.; Abela, A. R. *Org. Lett.* **2008**, *10*, 1333–1336.
(22) Lipshutz, B. H.; Taft, B. R. *Org. Lett.* **2008**, *10*, 1329–1332.

(23) Nishikata, T.; Abela, A. R.; Lipshutz, B. H. *Angew. Chem., Int. Ed.* **2010**, *49*, 781–784.
(24) Nishikata, T.; Lipshutz, B. H. *Org. Lett.* **2010**, *12*, 1972–1975.
(25) Mubofu, E. B.; Engberts, J. B. F. N. *J. Phys. Org. Chem.* **2007**, *20*, 764–770.
(26) Rispens, T.; Engberts, J. B. F. N. *J. Org. Chem.* **2002**, *67*, 7369–7377.
(27) Rispens, T.; Engberts, J. B. F. N. *J. Org. Chem.* **2003**, *68*, 8520–8528.
(28) The hydrolysis reactions used in the work presented here are not strictly uncatalyzed because one of the water molecules involved in the rate-determining step acts as a general-base catalyst. Here, however, catalysis by water provides an additional handle on the water concentration in the micellar Stern region
(29) Cordes, E. H.; Dunlap, R. B. *Acc. Chem. Res.* **1969**, *2*, 329–337.
(30) Bunton, C. A. *Catal. Rev.—Sci. Eng.* **1979**, *20*, 1–56.
(31) Buurma, N. J.; Serena, P.; Blandamer, M. J.; Engberts, J. B. F. N. *J. Org. Chem.* **2004**, *69*, 3899–3906.
(32) Buurma, N. J.; Herranz, A. M.; Engberts, J. B. F. N. *J. Chem. Soc., Perkin Trans. 2* **1999**, 113–119.
(33) Menger, F. M. *Acc. Chem. Res.* **1979**, *12*, 111–117.
(34) Vitha, M. F.; Dallas, A. J.; Carr, P. W. *J. Phys. Chem.* **1996**, *100*, 5050–5062.
(35) Vitha, M. F.; Weckwerth, J. D.; Odland, K.; Dema, V.; Carr, P. W. *J. Phys. Chem.* **1996**, *100*, 18823–18828.
(36) Mukerjee, P. *J. Phys. Chem.* **1962**, *66*, 943–945.
(37) Bunton, C. A.; Nome, F.; Quina, F. H.; Romsted, L. S. *Acc. Chem. Res.* **1991**, 24.
(38) Grieser, F.; Drummond, C. J. *J. Phys. Chem.* **1988**, *92*, 5580–5593.
(39) Jose, B. J.; Bales, B. L.; Peric, M. *J. Phys. Chem. B* **2009**, *113*, 13257–13262.
(40) Novaki, L. P.; El Seoud, O. A. *Phys. Chem. Chem. Phys.* **1999**, *1*, 1957–1964.
(41) Martins, C. T.; Lima, M. S.; El Seoud, O. A. *J. Phys. Org. Chem.* **2005**, *18*, 1072–1085.
(42) Soldi, V.; Keiper, J.; Romsted, L. S.; Cuccovia, I. M.; Chaimovich, H. *Langmuir* **2000**, *16*, 59–71.
(43) Romsted, L. S. *Langmuir* **2007**, *23*, 414–424.
(44) Cuccovia, I. M.; Agostinho-Neto, A.; Wendel, C. M. A.; Chaimovich, H.; Romsted, L. S. *Langmuir* **1997**, *13*, 5032–5034.
(45) Muñoz, M.; Rodríguez, A.; Del Mar Graciani, M.; Moyá, M. L. *Int. J. Chem. Kinet.* **2002**, *34*, 445–451.
(46) Buurma, N. J., Ph.D. Thesis, University of Groningen, Groningen, The Netherlands, 2003.
(47) Fife, T. H.; Jao, L. K. *J. Am. Chem. Soc.* **1969**, *91*, 4217–4220.
(48) Karzijn, W.; Engberts, J. B. F. N. *Tetrahedron Lett.* **1978**, *19*, 1787–1790.
(49) Engbersen, J. F. J.; Engberts, J. B. F. N. *J. Am. Chem. Soc.* **1975**, *97*, 1563–1568.
(50) Mooij, H. J.; Engberts, J. B. F. N.; Charton, M. *Recl. Trav. Chim. Pays-Bas* **1988**, *107*, 185–189.
(51) Bevington, P. R.; Robinson, K. D. *Data Reduction and Error Analysis for the Physical Sciences*, 3rd ed.; McGraw-Hill: New York, 2003.
(52) Atkinson, K. E. *An Introduction to Numerical Analysis*, 2nd ed.; Wiley: New York, 1988.
(53) Press, W. H.; Flannery, B. P.; Teukolsky, S. A.: Vetterling, W. T *Numerical Recipes in Pascal*; Cambridge University Press: Cambridge, U.K., 1990.
(54) Fernandez, M. A. S.; Fromherz, P. *J. Phys. Chem.* **1977**, *81*, 1755–1761.
(55) Wang, G.; Olofsson, G. *J. Phys. Chem.* **1995**, *99*, 5588–5596.
(56) Thevenot, C.; Grassl, B.; Bastiat, G.; Binana, W. *Colloids Surf. A: Physicochem. Eng. Aspects* **2005**, *252*, 105–111.
(57) Fuguet, E.; Ràfols, C.; Rosés, M.; Bosch, E. *Anal. Chim. Acta* **2005**, *548*, 95–100.
(58) van Os, N. M.; Haak, J. R.; Rupert, L. A. M. *Physico-Chemical Properties of Selected Anionic, Cationic and Nonionic Surfactants*; Elsevier: Amsterdam, 1993.
(59) Exner, O. *Correlation Analysis in Chemistry*; Plenum Press: London, 1978.
(60) Fadnavis, N.; Engberts, J. B. F. N. *J. Org. Chem.* **1982**, *47*, 152–154.
(61) Bunton, C. A.; Gillitt, N. D.; Mhala, M. M.; Moffatt, J. R.; Yatsimirsky, A. K. *Langmuir* **2000**, *16*, 8595–8603.
(62) Bunton, C. A. *J. Phys. Org. Chem.* **2005**, *18*, 115–120.
(63) Hammett, L. P. *Chem. Rev.* **1935**, *17*, 125–136.
(64) Hammett, L. P. *J. Am. Chem. Soc.* **1937**, *59*, 96–103.
(65) Otto, S.; Engberts, J. B. F. N. *Org. Biomol. Chem.* **2003**, *1*, 2809–2820.
(66) Engberts, J. B. F. N.; Blandamer, M. J. *J. Phys. Org. Chem.* **1998**, *11*, 841–846.
(67) Noordman, W. H.; Blokzijl, W.; Engberts, J. B. F. N.; Blandamer, M. J. *J. Org. Chem.* **1993**, *58*, 7111–7114.
(68) Reichardt, C. *Chem. Rev.* **1994**, *94*, 2319–2358.
(69) Silva, P. L.; Trassi, M. A. S.; Martins, C. T.; Seoud, O. A. E. *J. Phys. Chem. B* **2009**, *113*, 9512–9519.
(70) Zacharlasse, K. A.; Van Phuc, N.; Kozankiewicz, B. *J. Phys. Chem.* **1981**, *85*, 2676–2683.
(71) Asaad, N.; Otter, M. J. D.; Engberts, J. B. F. N. *Org. Biomol. Chem.* **2004**, *2*, 1404–1412.
(72) Menger, F. M. *Acc. Chem. Res.* **1979**, *12*, 111–117.
(73) Hawrylak, B. E.; Marangoni, D. G. *Can. J. Chem.* **1999**, *77*, 1241–1244.
(74) Fendler, J. H.; Patterson, L. K. *J. Phys. Chem.* **1971**, *75*, 3907.
(75) Blandamer, M. J.; Engberts, J. B. F. N.; Gleeson, P. T.; Reis, J. C. R. *Chem. Soc. Rev.* **2005**, *34*, 440–458.
(76) Angeli, A. D.; Cipiciani, A.; Germani, R.; Savelli, G.; Cerichelli, G.; Bunton, C. A. *J. Colloid Interface Sci.* **1988**, *121*, 42–48.
(77) Rispens, T.; Cabaleiro-Lago, C.; Engberts, J. B. F. N. *Org. Biomol. Chem.* **2005**, *3*, 597–602.
(78) Bunton, C. A.; Huang, S. K. *J. Org. Chem.* **1972**, *37*, 1790–&.
(79) De Albrizzio, J. P.; Cordes, E. H. *J. Colloid Interface Sci.* **1979**, *68*, 292–294.
(80) Tada, E. B.; Novaki, L. P.; El Seoud, O. A. *Langmuir* **2001**, *17*, 652–658.
(81) Possidonio, S.; Siviero, F.; El Seoud, O. A. *J. Phys. Org. Chem.* **1999**, *12*, 325–332.
(82) Buurma, N. J.; Pastorello, L.; Blandamer, M. J.; Engberts, J. B. F. N. *J. Am. Chem. Soc.* **2001**, *123*, 11848–11853.
(83) Benak, H.; Engberts, J. B. F. N.; Blandamer, M. J. *J. Chem. Soc., Perkin Trans. 2* **1992**, 2035–2038.
(84) Blandamer, M. J.; Blundell, N. J.; Burgess, J.; Cowles, H. J.; Engberts, J. B. F. N.; Horn, I. M.; Warrick, P., Jr. *J. Am. Chem. Soc.* **1990**, *112*, 6854–6858.
(85) Blokzijl, W.; Blandamer, M. J.; Engberts, J. B. F. N. *J. Org. Chem.* **1991**, *56*, 1832–1837.
(86) El Seoud, O. A.; Ruasse, M. F.; Possidonio, S. *J. Phys. Org. Chem.* **2001**, *14*, 526–532.
(87) Noordman, W. H.; Blokzijl, W.; Engberts, J. B. F. N.; Blandamer, M. J. *J. Chem. Soc., Perkin Trans. 2* **1995**, 1411–1414.
(88) Bales, B. L.; Messina, L.; Vidal, A.; Peric, M.; Nascimento, O. R. *J. Phys. Chem. B* **1998**, *102*, 10347–10358.